Journal of Thermal Science Vol.28, No.2 (2019) 195−203

https://doi.org/10.1007/s11630-019-1076-x **Article ID: 1003-2169(2019)02-0195-09**

Energy Storage Performance of a PCM in the Solar Storage Tank

MAO Qianjun*, CHEN Hongzhang, YANG Yizhi

School of Urban Construction, Wuhan University of Science and Technology, Wuhan 430065, China.

Abstract: High-temperature solar thermal power station with solar energy storage is one of the effective ways to solve energy shortage and environmental pollution. The heat storage characteristics of phase change materials in solar energy storage tanks directly affect the performance of the system and its future promotion and utilization. Based on the knowledge of heat transfer, fluid mechanics and engineering thermodynamics, this paper uses MATLAB software to compile the dynamic heat storage characteristics calculation program of phase change materials in energy storage tanks, and verify the results. This paper analyzes the phase change heat storage process with three PCM initial temperatures and three HTF speeds. The results show that when the initial temperature of the PCM changes from 185°C to 210°C, the latent heat storage heat increases by 21.8%, and the total heat storage decreases. Increasing the HTF speed from 1.8 m/s to 2.2 m/s, the melting time was reduced from 414 minutes to 390 minutes, and the total heat storage and sensible heat storage were also increased. The results also show that changing the initial temperature of the PCM and the flow rate of the HTF will change the thermal storage performance of the system. The research has certain reference significance for mastering the basic principle of high temperature solar thermal power generation system and promoting the application of the system.

Keywords: solar phase change materials, energy storage performance, sensible heat, latent heat

1. Introduction

In recent years, due to a series of problems caused by abusive fossil energy, such as environmental pollution, greenhouse effect, etc., the application of renewable energy has been required. Solar energy, which is a clean and abundant new energy source, has broad application prospects [1,2]. Although it is difficult to use solar energy in a stable and efficient manner under natural conditions, CSP technology can solve this problem effectively [3-6]. Meanwhile, research on phase change thermal storage systems will help improve energy use, especially for solar energy utilization [7,8].

In order to find more economical and feasible way of phase change heat storage, the researchers have done much outstanding work. Some researchers focus on the experimental investigation for the heat storage performance of the CSP plant. Yang et al. [9] have investigated the thermal characteristics of a shell-and-tube latent heat storage (LHS) unit. Ma et al. [10] have researched the thermal performance of high temperature LHS system by using annular fins. Diao et al. [11] have experimentally investigated the effects of different HTF inlet temperatures and volume flow rates on the PCM temperature. Li et al. [12] have researched the heat storage performance of a new high-temperature packed-bed thermal energy storage (TES) system with macro-encapsulation molten salt. Tiari et al. [13] have studied the effects of different HTF temperatures and flow rates on the thermal performance of the LHS system. Abdulateef et al. [14] have investigated

Received: June 3, 2018 Associate editor: PENG Jinqing Corresponding author: MAO Qianjun E-mail: maoqianjun@163.com

Nomenclature

c_p	Specific heat/J·kg^{-1}·K^{-1}	Q	The amount of energy/J
CSP	Concentrating Solar Power	R	Thermal resistance/K·W^{-1}
d_1	The inside diameter of the model/mm	r	Radius of the storage tank/m
d_2	The outer diameter of the model/mm	T	Temperature/°C
E	The amount of heat/J	u	Fluid velocity/m·s^{-1}
h	Convection heat transfer coefficient /W·m^{-2}·K^{-1}	z	Axial length/m
HTF	Heat transfer fluid	δ	The thickness of heat exchanger pipe/mm
L	Latent heat/J·kg^{-1}	λ	Thermal conductivity of the material /W·m^{-1}·K^{-1}
l	The length of the model/mm	μ	Kinematic viscosity/N·s·m^{-2}
M	Mass/kg	ρ	Density of the material/kg·m^{-3}
PCM	Phase change materials	v	Dynamic viscosity coefficient/m^2·s^{-1}

an experimental system by using a horizontal triplex tube heat exchanger with internal longitudinal fins incorporating PCM. Amagour et al. [15] have also researched a latent heat storage system.

In addition, many references have numerically studied the ways to enhance heat transfer performance of CSP plant. Lu et al. [16] have studied the performance of a water storage tank which has two kinds of PCMs. Bie et al. [17] have studied the effects of the PCMs on storage energy performance. Niyas et al. [18] have investigated a novel way consisting of tube-in-tube LHS system with a very small inner tube. Riahi et al. [19] have studied the changes of different shell and tube configurations on the characteristics and behavior of PCM. Cheng et al. [20] have put forward a cascaded packed bed cool thermal energy storage unit. Parsazadeh et al. [21] have studied a multi-scale heat transfer enhancement technique. Nithyanandam et al. [22] have also investigated the transient charge and discharge performance.

The phase change heat storage process has two contributions: LHS and sensible heat storage (SHS). When studying the thermal storage performance of the system, considering these two parts together will have more accurate result. However, in the current research, most researchers have mainly concentrated on the latent heat storage part of the PCM in the heat storage process, and paid insufficient attention to the sensible heat storage. These less-than-perfect researches may result from the complication of phase transition process. Since phase and temperature change at the same time, it is difficult to calculate the stored heat in the phase change process. Under normal circumstances, the calculation of the phase change heat storage temperature is based on the HTF temperature change. This paper proposes a calculation method that considers the PCM temperature change. The new method has been proposed to calculate the system heat storage amount based on the thermal storage unit. In contrast, the calculation method of this paper is more accurate. Through this method, the total heat storage capacity of the system has been calculated. Moreover, latent heat capacity and sensible heat capacity during the heat storage process have been calculated separately. The complex phase change heat storage is split into two relatively simple processes, reducing the complexity of the phase change heat storage process, and further studying the change of heat storage performance in the phase change process. This paper has provided a novel method to study heat storage performance changes of the system during phase change heat storage process and a new idea for numerical calculation of phase change heat storage process.

2. Physical Model and Governing Equations

2.1 Physical model

In this paper, a cylindrical phase change thermal energy storage model has been established. PCM temperature field in the model has high symmetry, which can simplify the calculation and improve the accuracy of the research results. The model has good thermal conductivity, thus can increase the heat transfer efficiency of the system, and can store more PCM, which has high application value. The axial section is shown in Fig. 1. HTF flows in the inner of heat transfer tube, and the PCM is between heat transfer tube and shell. The tube in this model is 1000 mm long (l). And, its inside diameter (d_1) and outside diameter (d_2) are 100 mm and 200 mm respectively. Besides the thickness of the inner tube (δ) is 1 mm. In this model, the HTF is water vapor with 550°C inlet temperature, and the PCM is mixture of molten salts consisting of 54% KNO_3 and 46% $NaNO_3$. Latent heat value L is 69.75 kJ/kg. Phase transition temperature T_m is 220°C and initial temperature is T_0. Thermal-physical parameters about PCM, HTF and the inner tube are shown in Table 1.

To simplify the calculation, we have set several preconditions as follows:

(1) Volume expansion and flow of PCM after melting can be ignored.

(2) The convection heat transfer of the PCM is not considered.

(3) Except for the wall of the inner tube, other outer walls of the model are regarded as adiabatic boundaries.

(4) Due to the symmetry of this model, only one-half of axial section needs to be calculated.

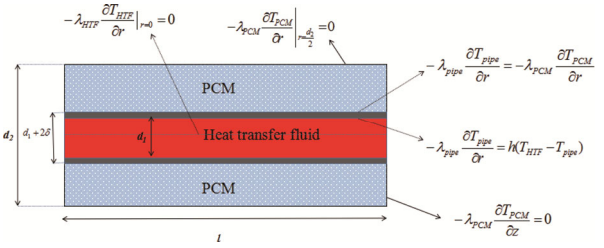

Fig. 1 The schematic of heat transfer model

2.2 Governing equations

According to heat conduction equation in cylindrical coordinate system, the temperature fields of HTF and PCM have been solved respectively [23,24]. The corresponding equations are shown as follows:

For HTF area

$$\begin{aligned}&\frac{T^{n+1}{}_{i,j}-T^{n}{}_{i,j}}{\Delta t}+u\frac{T^{n}{}_{i+1,j}-T^{n}{}_{i,j}}{\Delta z}\\&=\frac{T^{n}{}_{i+1,j}-T^{n}{}_{i,j}}{\rho c_p\Delta z R_{up}}+\frac{T^{n}{}_{i-1,j}-T^{n}{}_{i,j}}{\rho c_p\Delta z R_{down}}\\&+\frac{T^{n}{}_{i,j+1}-T^{n}{}_{i,j}}{2\pi r\Delta r\rho c_p R_{r+dr}}+\frac{T^{n}{}_{i,j-1}-T^{n}{}_{i,j}}{2\pi r\Delta r\rho c_p R_{r-dr}}\\&+\frac{u}{c_p}\left(\frac{u^{n}{}_{i,j+1}-u^{n}{}_{i,j-1}}{2\Delta r}\right)^2\end{aligned} \tag{1}$$

Table 1 Thermal-physical properties in the model

	HTF	Tube	PCM
Thermal Conductivity λ /W·m^{-1}·K^{-1}	0.061	54	0.5 (Solid)/0.3 (Liquid)
Specific heat capacity c_p /J·kg^{-1}·K^{-1}	2170	460	1420 (Solid)/1500 (Liquid)
Density ρ /kg·m^{-3}	0.266	7850	2040 (Solid)/1950 (Liquid)
Kinematic viscosity μ /N·s·m^{-2}	2.87×10^{-5}	——	——
Dynamic viscosity coefficient v /m^2·s^{-1}	1.0807×10^{-4}	——	——

where n is the number of time nodes; i is the axial grid position; j is the radial grid position; Δt is the tiny interval of time; Δz is the amount of change in axial direction; Δr is the amount of change in the radial direction; u is the HTF flow speed; R is the thermal resistance.

For PCM area:

$$\begin{aligned}\frac{T^{n+1}{}_{i,j}-T^{n}{}_{i,j}}{\Delta t}&=\frac{T^{n}{}_{i+1,j}-T^{n}{}_{i,j}}{\rho c_p\Delta z R_{up}}+\frac{T^{n}{}_{i-1,j}-T^{n}{}_{i,j}}{\rho c_p\Delta z R_{down}}\\&+\frac{T^{n}{}_{i,j+1}-T^{n}{}_{i,j}}{2\pi r\Delta r\rho c_p R_{r+dr}}+\frac{T^{n}{}_{i,j-1}-T^{n}{}_{i,j}}{2\pi r\Delta r\rho c_p R_{r-dr}}\end{aligned} \tag{2}$$

The phase change process has been estimated by:

For thermal storage unit with a mass of d_M, when it reaches the phase transition temperature, the heat, required to complete phase change process is:

$$Q_0 = Ld_M \tag{3}$$

In this study, the amount of heat, absorbed by the thermal storage unit after reaching T_m, can be accumulated and expressed as:

$$Q=\sum_{f=1}^{F}\left(C_P d_M\Delta T_f\right)=d_M\sum_{f=1}^{F}\left(C_P\Delta T_f\right)\quad F=1, 2, 3\ldots \tag{4}$$

where f is a time step; F is the amount of time step; ΔT_f is the temperature change in the thermal storage unit within one time step.

When Q exceeds Q_0, the phase change process is over. Otherwise, the phase change process is not over.

2.3 Calculation of heat storage

2.3.1 Calculating the heat storage for only one state

Fig. 2 has shown two different temperature fields in PCM with only one state. Fig. 2(a) shows solid state of PCM. In this case, the maximum temperature of PCM is lower than the phase transition temperature. The heat storage can be expressed as:

$$E = c_{ps}M\left(\overline{T}-T_0\right) \tag{5}$$

where E is the heat storage; M is the mass of the PCM; c_{ps} is the specific heat capacity of phase change material under solid state; $\overline{T}$ is the average temperature of the PCM.

Fig. 2(b) has shown the temperature field in which PCM has completely melted. The PCM minimum temperature is higher than the phase transition temperature. Under the condition, the heat storage can be expressed as Eq. (6) [25]:

$$E = M\left[\left(\overline{T}-T_m\right)c_{pl}+L+\left(T_m-T_0\right)c_{ps}\right] \tag{6}$$

where c_{pl} is the specific heat capacity of phase change material under liquid state.

2.3.2 Calculating the heat storage for two states

Fig. 3 has shown temperature field and state distribution of the PCM with two states. In this case, the phase transition temperature is between the maximum and minimum temperatures of PCM. For regions where temperature excels the phase transition temperature, the melting process has ended, as shown in area 1 in Fig. 3(b).

For regions where the PCM temperature is inferior to phase transition temperature, the melting process has not yet started, as shown in area 2 in Fig. 3(b). While the temperature of the PCM reaches the phase transition temperature, the melting of PCM is still in process, such as the area between the 1 and 2 regions in Fig. 3(b). Since there are three regions for PCM with uneven distribution and different degrees of phase change process, it is difficult to calculate the heat storage for the latent thermal storage system by using the temperature of PCM.

To calculate the heat storage of phase change process, a new method, based on thermal storage unit, has been proposed in this paper. For a thermal storage unit with a mass of d_M, it will pass through three parts in a complete phase change process: the melting phase has not started, the melting phase in process, and the melting phase has completed.

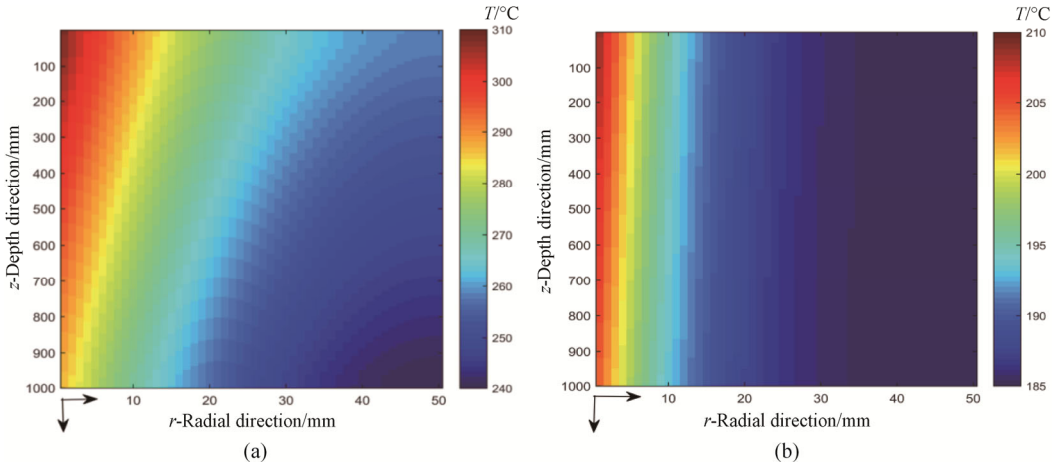

Fig. 2 The temperature field of PCM

Taking one time step as the calculation cycle, firstly, the program estimates the state of the thermal storage unit, and then calculates the amount of stored heat in thermal storage unit in the calculation cycle via corresponding formula. The total heat storage capacity of the thermal storage unit can be obtained by accumulating heat storage for multiple calculation cycles. Dividing the phase change material into a number of heat storage units, and then summing up the heat storage capacity of each heat storage unit, the heat storage capacity of the system during the heat storage process can be calculated.

The formula is expressed as:

$$Q_{i,j}=\begin{cases}\sum_{f=1}^{F}\left(c_{ps}\Delta T_f d_M\right), & T_{i,j}<T_m\\ \left(T_m-T_0\right)c_{ps}d_M+\sum_{f=1}^{F}\left(c_{ps}\Delta T_f d_M\right), & T_{i,j}=T_m\\ \left(T_m-T_0\right)c_{ps}d_M+Ld_M+\sum_{f=1}^{F}\left(c_{pl}\Delta T_f d_M\right), & T_{i,j}>T_m\end{cases} \tag{7}$$

$$E=k\sum_{i=1,j=1}^{m,n}Q_{i,j} \tag{8}$$

where m, n are the grid number in the model; $Q_{i,j}$ is the heat storage of the unit; E is the total heat storage of the model; k is the amount of the section.

2.3.3 Calculating the sensible heat capacity and latent heat capacity

Phase change heat storage is a complex process, but the complex process can be simplified by splitting it into two simple processes: latent heat storage and sensible heat storage. By calculating the latent heat storage capacity and the sensible heat storage heat quantity of the system, the change of the heat storage performance during the phase change heat storage process can be studied, and the phase change heat storage process can be further studied. Based on the calculation method of system storage heat, we have proposed a method that has

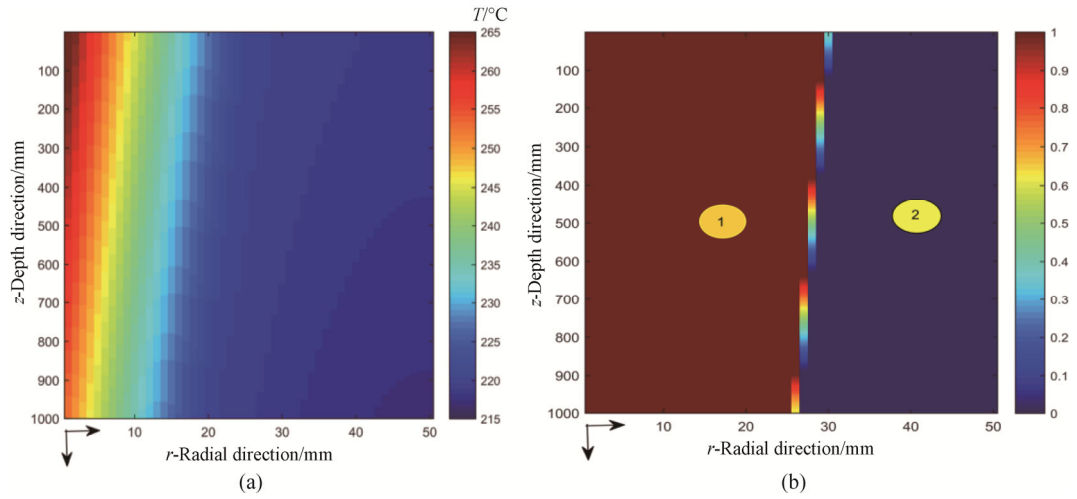

Fig. 3 The temperature field and state distribution of PCM

calculated the sensible heat capacity and latent heat capacity in melting progress, as follows:

Sensible heat capacity:

$$Q_{Si,j}=\begin{cases}\sum_{f=1}^{F}\left(c_{ps}\Delta T_f d_M\right), & T_{i,j}<T_m\\ \left(T_m-T_0\right)c_{ps}d_M, & T_{i,j}=T_m\\ \left(T_m-T_0\right)c_{ps}d_M+\sum_{f=1}^{F}\left(c_{pl}\Delta T_f d_M\right), & T_{i,j}>T_m\end{cases} \quad (9)$$

$$E_S=k\sum_{i=1,j=1}^{m,n}Q_{Si,j} \quad (10)$$

where $Q_{Si,j}$ is the sensible heat capacity of the thermal storage unit; E_S is the sensible heat capacity of the model.

Latent heat capacity:

$$Q_{Li,j}=\begin{cases}0, & T_{i,j}<T_m\\ \sum_{f=1}^{F}\left(c_{ps}\Delta T_f d_M\right), & T_{i,j}=T_m\\ Ld_M, & T_{i,j}>T_m\end{cases} \quad (11)$$

$$E_L=k\sum_{i=1,j=1}^{m,n}Q_{Li,j} \quad (12)$$

where $Q_{Li,j}$ is the latent heat capacity of the thermal storage unit; E_L is the latent heat capacity of the model.

3. Model Validation

The computer code of this study has been written by C language in MATLAB software. The correctness of the code has been verified in literature [21]. To guarantee the reliability of the method that has calculated heat storage in this paper, we has calculated the total heat storage at the same time by using the methods proposed in reference [25] and this study respectively. These calculations show that the variation between these two ways is about 0.2%, which agrees well with each other, as shown in Fig. 4.

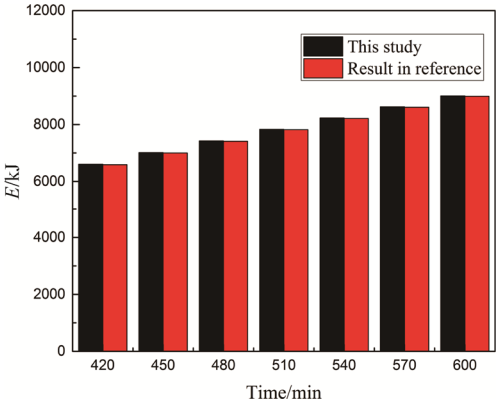

Fig. 4 The validation of calculation method in this study

4. Results and Analysis

4.1 Phase change progress analysis

Fig. 5 shows the liquid fraction of PCM in this model. The initial temperature of PCM is 185°C, and the velocity of HTF is 2.0 m/s. When the charging time has reached 46 min, the PCM begins to melt. While the charging time has reached 510 min, the liquid fraction becomes 1, which means the phase change progress is over.

Fig. 6 is the heat storage of melting process. The whole process can be divided into three stages. The first stage is that only sensible heat storage exists and the liquid fraction is zero. The second stage is that the sensible heat storage and latent heat storage exist at the same time. But it is significant to note that PCM do not melt when the latent heat storage started. In this process, the PCM starts to melt at about 46 min, while the latent heat storage starts about 33 min. The different time has shown the strong heat storage capacity of phase change heat storage. The third stage is that latent heat storage is over and only sensible heat storage exists. The liquid fraction reaches 1 and the PCM completely becomes

liquid. When the melting process is over, the heat capacity is about 8184 kJ consisting of latent heat capacity about 3356 kJ and sensible heat capacity about 4828 kJ. Due to different temperature between the PCM and the HTF, the sensible heat storage will continue to increase until the difference of temperature decreasing to zero.

The heat storage rate of the phase change heat storage process has been shown in Fig. 7. At the beginning of the process, the total heat storage and sensible heat storage has reached the maximum, which is about 355.56 J/s. Since phase change does not start, the latent heat storage rate is zero. At the second stage, with the reduction of

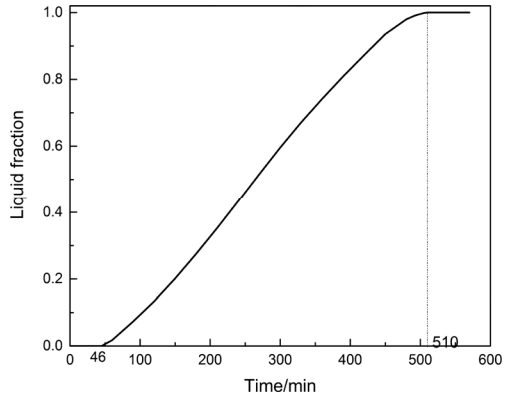

Fig. 5 The liquid fraction of the heat storage progress

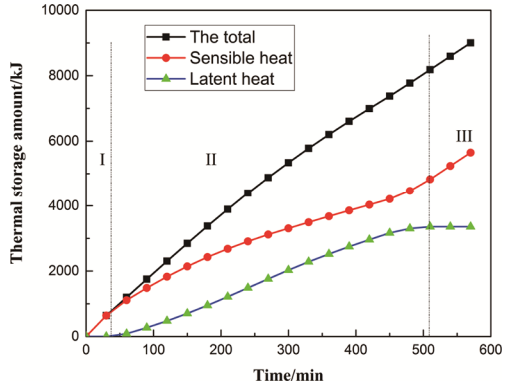

Fig. 6 The heat storage of the phase change process

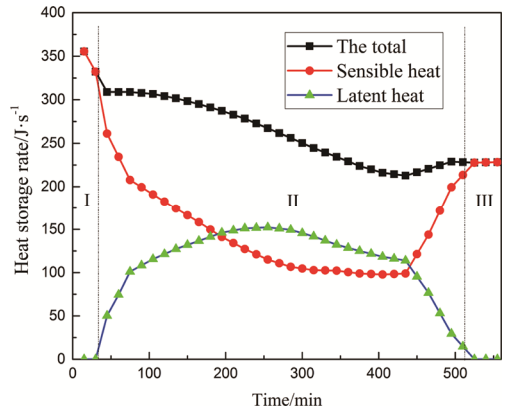

Fig. 7 The heat storage rate of the phase change process

different temperature between PCM and HTF, the total heat storage rate and the sensible heat storage rate have been falling until the charging time is about 450 min. The sensible heat storage rate has a significant decline, when the latent heat storage started, which means that latent heat storage process has limited sensible heat storage performance to a remarkable extent. Then, they have both risen to 227.78 J/s. The total heat storage rate has increased about 12.78 J/s and sensible heat storage rate has added about 128.89 J/s. The liquid fraction of the PCM has changed from 0.97 to 1. During this stage, the latent heat storage rate gradually has increased from 0 to 152.22 J/s when the charging time changes from 33 min to 270 min. With process continuing, the latent heat storage rate will reduce to zero when PCM completely becomes liquid. In the third stage, the latent heat storage rate is zero, and the total heat storage rate and the sensible heat storage rate have become equal and kept constant during a period of time.

4.2 PCM initial temperature analysis

To study the relevance between latent heat and sensible heat in melting process, we have calculated three different phase change storage process in which PCM has three different initial temperatures, which are 185°C, 200°C and 210°C. Meanwhile, HTF velocity keeps 2 m/s.

The effects of PCM initial temperature on liquid fraction in melting process has been shown in Fig. 8. When the initial temperature increases from 185°C to 210°C, the time of phase change will decrease from 510 min to 401 min. This ratio of reduction is about 21.8%. When the difference between PCM initial temperature and transition temperature, has reduced from 25°C to 10°C, the latent heat process has been enhanced 21.8%. But does the heat storage performance of the model actually improve?

Figs. 9-11 have shown the effects of different PCM initial temperatures on the heat storage of the model. Due to more easy to reach the transition temperature, the phase change process with the 210°C initial temperature has the best latent heat storage performance, as shown in Fig. 9. On the other hand, smaller temperature difference will weaken the sensible heat storage of process. A conclusion can be drawn from Fig. 10 that sensible heat capacity reduces with PCM initial temperature increasing. Although latent heat storage has been enhanced, the sensible heat storage performance has been decreased. The sensible heat storage performance boosts when melting process is about to end. Considering sensible heat storage and latent heat storage comprehensively, the process with 185°C initial temperature has a better heat storage performance, as shown in Fig. 11. Consequently, sensible heat storage cannot be ignored when studying phase change heat storage performance.

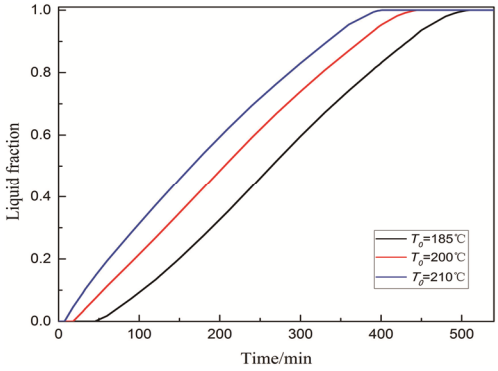

Fig. 8 Effect of PCM initial temperature on liquid fraction

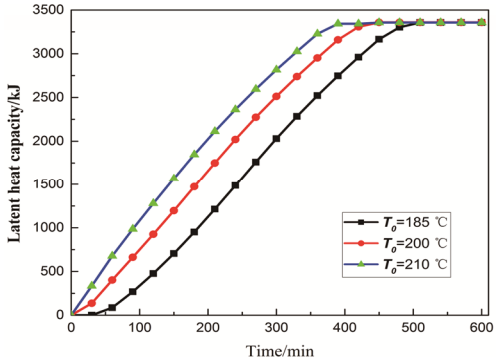

Fig. 9 Latent heat storage of different PCM initial temperature

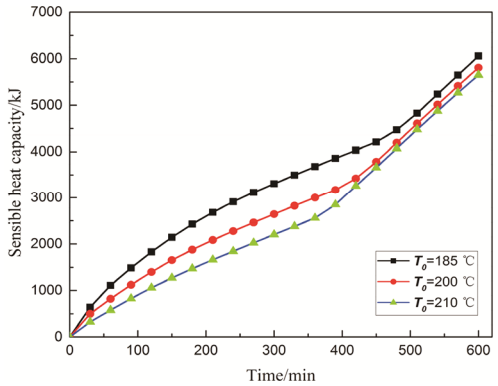

Fig. 10 Sensible heat storage of different PCM initial temperature

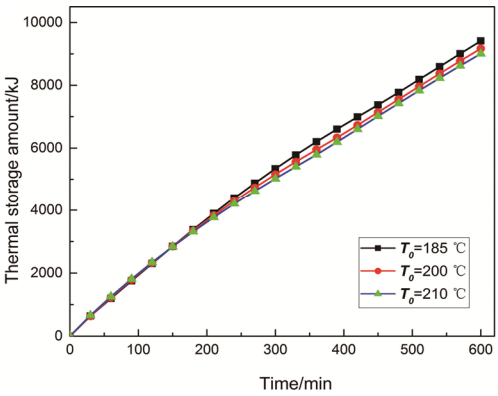

Fig. 11 Total heat storage of different PCM initial temperature

4.3 HTF velocity analysis

Figs. 12-15 have showed the effects of HTF velocity on the phase change heat storage process. The initial temperature of PCM keeps 210°C. The HTF speeds have varied from 1.8 m/s, 2.0 m/s and 2.2 m/s. When the HTF velocity has increased from 1.8 m/s to 2.2 m/s, the melting time has been reduced from 414 min to 390 min. The latent heat storage performance has increased about 5.8%, as shown in Fig. 12 and Fig. 13. The sensible heat storage under different HTF speeds has been shown in Fig. 14. Before the charging time reaches 350 min, the sensible heat storage is closed. And the liquid fraction of three conditions is 0.9703, 0.9541 and 0.9355, respectively. The melting process is almost ready to finish. This indicates that during the melting process, changes in HTF speed have little effect on sensible heat storage. While the process continues, the difference has obviously increased. The sensible heat storage performance has been improved with the increasing of HTF velocity when the melting process is finished. The total heat storage under the different HTF speeds is shown in Fig. 15. The differences among the three conditions are not obvious until the charging time is longer than 300 min. The progress with faster HTF velocity has better phase

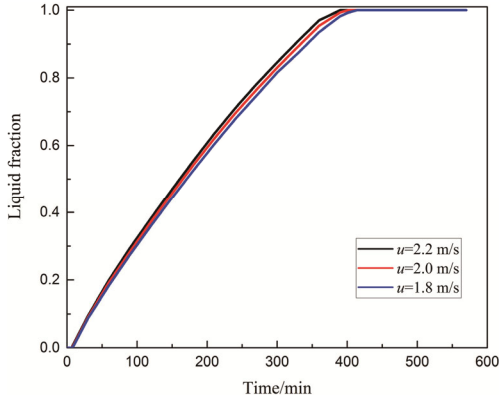

Fig. 12 The liquid fraction of different HTF velocity

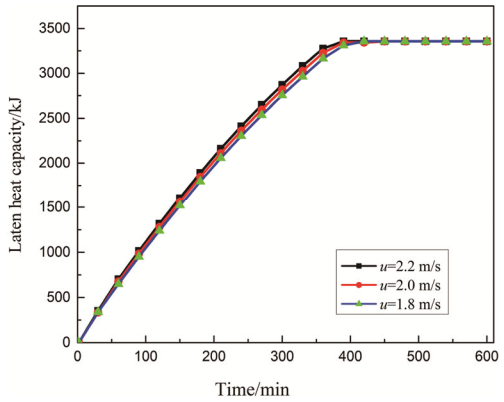

Fig. 13 The latent heat storage of different HTF velocity

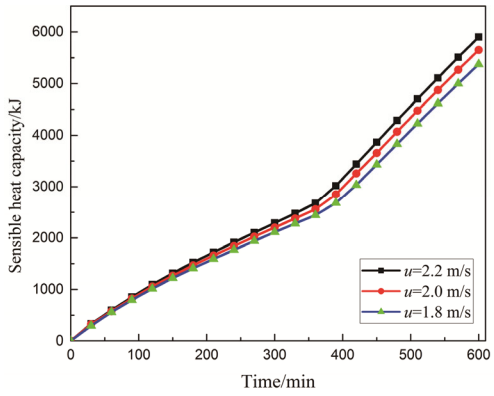

Fig. 14 The sensible heat storage of different HTF velocity

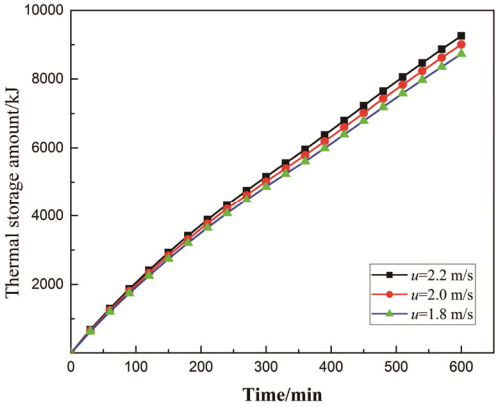

Fig. 15 The total heat storage of different HTF velocity

change heat storage performance. And according to the study on the latent heat storage and sensible heat storage, the enhancement of total heat storage has been mainly caused by sensible heat storage performance strengthening.

5. Conclusions

In this study, based on heat storage unit considerations, a new method to calculate the heat storage for the phase change heat storage process has been proposed. The sensible heat capacity and the latent heat capacity during the phase change heat storage process can be calculated as well. According to the new method, the heat storage processes with three different PCM initial temperatures and three different HTF speeds have been analyzed. The conclusions can be obtained as:

Increasing PCM initial temperature from 185°C to 210°C, melting time reduces from 510 min to 401 min. The process with higher PCM initial temperature has better latent heat storage performance and worse sensible heat storage performance. The calculation also has shown that latent heat storage process limits sensible heat storage performance until the melting process ends.

Improving the HTF velocity can enhance the thermal storage performance. When changing HTF velocity from 1.8 m/s to 2.2 m/s, the latent heat performance has been increased 5.8%. However, the result has shown that the enhancement of the total heat storage is mainly caused by sensible heat storage performance strengthening.

The new method which has been proposed in this study, used to calculate the absorbed heat, can be used to study heat storage performance changes of the system during phase change thermal storage process.

Acknowledgements

This work was supported by the National Natural Science Foundation of China (Grant Nos. 51876147 and 51406033).

References

[1] Rajendran D.R., Sundaram E.G., Jawahar P., Experimental studies on the thermal performance of a parabolic dish solar receiver with the heat transfer fluids SiC plus water nano fluid and water. Journal of Thermal Science, 2017, 26(3): 263–272.

[2] Amina B., Miloud A., Samir L., Abdelylah B., Solano J.P., Heat transfer enhancement in a parabolic trough solar receiver using longitudinal fins and nanofluids. Journal of Thermal Science, 2016, 25(5): 410–417.

[3] Mao Q.J, Zhang L.Y, Wu H.J., Charge time of the storage material of the tank for a solar power plant. International Journal of Hydrogen Energy, 2016, 41(35): 154646–154650.

[4] Li G.Q, Zhang G., He W., Ji J., Lv S., Chen X., Chen H.B., Performance analysis on a solar concentrating thermoelectric generator using the micro-channel heat pipe array. Energy Conversion and Management, 2016, 112(15): 191–198.

[5] Lv S., He W., Hu D.Y., Zhu J., Li G.Q., Chen H.B., Liu M.H., Study on a high-performance solar thermoelectric system for combined heat and power. Energy Conversion and Management, 2017, 143(1): 459–469.

[6] Li Q., Bai F.W., Yang B., Wang Y., Xu L., Chang Z.S., Wang Z.F., Hefni B.E., Yang Z.Q., Kubo S., Kiriki H., Han M.X., Dynamic simulations of a honeycomb ceramic thermal energy storage in a solar thermal power plant using air as the heat transfer fluid. Applied Thermal Engineering, 2018, 129: 636–645.

[7] Wang F.Q., Cheng Z.M., Tan J.Y., Yuan Y., Yong S., Liu L.H., Progress in concentrated solar power technology with parabolic trough collector system: a comprehensive review. Renewable and Sustainable Energy Reviews, 2017, 79: 1314–1328.

[8] Wang F.Q., Lai Q.Z., Han H.Z., Tan J.Y., Parabolic trough receiver with corrugated tube for improving heat

transfer and thermal deformation characteristics. Applied Energy, 2016, 164: 411–424.

[9] Yang J.L., Yang L.J., Xu C., Du X.Z., Experimental study on enhancement of thermal energy storage with phase change material. Applied Energy, 2016, 169(1): 164–176.

[10] Ma Z., Yang W.W., Yuan F., Jin B., He Y.L., Investigation on the thermal performance of a high-temperature latent heat storage system. Applied Thermal Engineering, 2017, 122(25): 579–592.

[11] Diao Y.H., Kang Y.M., Liang L., Zhao Y.H., Zhu T.T., Experimental investigation on the heat transfer performance of a latent thermal energy storage device based on flat miniature heat pipe arrays. Energy, 2017, 138(1): 929–934.

[12] Li M.J., Jin B., Ma Z., Yuan F., Experimental and numerical study on the performance of a new high temperature packed-bed thermal energy storage system with macro encapsulation of molten salt phase change material. Applied Energy, 2018, 221(1): 1–15.

[13] Tiari S., Mahdavi M., Qiu S.G., Experimental study of a latent heat thermal energy storage system assisted by a heat pipe network. Energy Conversion and Management, 2017, 153(1): 362–373.

[14] M. Abdulateef A., Mat S., Sopian K., Abdulateef J., A. Gitan A., Experimental and computational study of melting phase change material in a triplex tube heat exchanger with longitudinal/triangular fins. Solar Energy, 2017, 155: 142–153.

[15] Amagour M.E.H., Rachek A., Bennajah M., Touhami M.E., Experimental investigation and comparative performance analysis of a compact finned-tube heat exchanger uniformly filled with a phase change material for thermal energy storage. Energy Conversion and Management, 2018, 165(1): 137–151.

[16] Lu S.L., Zhang T.S., Chen Y.F., Study on the performance of heat storage and heat release of waterstorage tank with PCMs. Energy and Buildings, 2018, 150(1): 1770–1780.

[17] Bie Y., Li M., Malekian R., Chen F., Feng Z.K., Li Z.X., Effect of phase transition temperature and thermal conductivity on the performance of Latent Heat Storage System. Applied Thermal Engineering, 2018, 135(5): 218–227.

[18] Niyas H., Muthukumar P., A novel heat transfer enhancement technique for performance improvements in encapsulated latent heat storage system. Solar Energy, 2018, 164: 276–286.

[19] Riahi S., Y. Saman W., Bruno F., Belusko M., Tay N.H.S., Performance comparison of latent heat storage systems comprising plate fins with different shell and tube configurations. Applied Energy, 2018, 212(15): 1095–1106.

[20] Cheng X.W., Zhai X.Q., Thermal performance analysis and optimization of a cascaded packed bed cool thermal energy storage unit using multiple phase change materials. Applied Energy, 2018, 215(1): 566–576.

[21] Parsazadeh M., Duan X., Numerical study on the effects of fins and nanoparticles in a shell and tube phase change thermal energy storage unit. Applied Energy, 2018, 216(15): 142–156.

[22] Nithyanandam K., Barde A., Lakeh R.B., Wirz R.E., Charge and discharge behavior of elemental sulfur in isochoric high temperature thermal energy storage systems. Applied Energy, 2018, 214(15): 166–177.

[23] Mao Q.J., Chen H.Z., Zhao Y.Z., Wu H.J., A novel heat transfer model of a phase change material using in solar power plant. Applied Thermal Engineering, 2018, 129(25): 557–563.

[24] Mao Q.J., Recent developments in geometrical configurations of thermal energy storage for concentrating solar power plant. Renewable and Sustainable Energy Reviews, 2016, 59: 320–327.

[25] Kuravi S., Trahan J., Goswami D.Y., Muhammad M.R., Stefanakos E.K., Thermal energy storage technologies and systems for concentrating solar power plants. Progress in Energy and Combustion Science, 2013, 39(4): 285–319.